ELSEVIER

International Journal of Refrigeration 26 (2003) 749–757

REVUE INTERNATIONALE DU FROID
INTERNATIONAL JOURNAL OF
refrigeration

www.elsevier.com/locate/ijrefrig

Waste heat driven dual-mode, multi-stage, multi-bed regenerative adsorption system

B.B. Saha[a,*], S. Koyama[a,1], T. Kashiwagi[b], A. Akisawa[b], K.C. Ng[c], H.T. Chua[c]

[a]*Institute for Materials Chemistry and Engineering, Kyushu University, Kasuga-koen 6-1, Kasuga-shi, Fukuoka 816-8580, Japan*
[b]*Bio Applications and Systems Engineering, Tokyo University of Agriculture & Technology, 2-24-16 Naka-machi, Koganei-shi, Tokyo 184-8588, Japan*
[c]*Department of Mechanical Engineering, National University of Singapore 10, Kent Ridge Crescent, 119260 Singapore*

Received 16 December 2002; received in revised form 2 May 2003; accepted 2 May 2003

Abstract

Over the past few decades there have been considerable efforts to use adsorption (solid/vapor) for cooling and heat pump applications, but intensified efforts were initiated only since the imposition of international restrictions on the production and utilization of CFCs and HCFCs. In this paper, a dual-mode silica gel–water adsorption chiller design is outlined along with the performance evaluation of the innovative chiller. This adsorption chiller utilizes effectively low-temperature solar or waste heat sources of temperature between 40 and 95 °C. Two operation modes are possible for the advanced chiller. The first operation mode will be to work as a highly efficient conventional chiller where the driving source temperature is between 60 and 95 °C. The second operation mode will be to work as an advanced three-stage adsorption chiller where the available driving source temperature is very low (between 40 and 60 °C). With this very low driving source temperature in combination with a coolant at 30 °C, no other cycle except an advanced adsorption cycle with staged regeneration will be operational. The drawback of this operational mode is its poor efficiency in terms of cooling capacity and COP. Simulation results show that the optimum COP values are obtained at driving source temperatures between 50 and 55 °C in three-stage mode, and between 80 and 85 °C in single-stage, multi-bed mode.

Keywords: Adsorption; Adsorption system; Heat recovery; Silica gel

Système à adsorption multiétagé à régénération cyclique, à partir de chaleur perdue

Mots clés : Adsorption ; Système à adsorption ; Récupération de chaleur ; Gel de silice

1. Introduction

The severity of the ozone layer destruction problem due to CFCs and HCFCs has been calling for rapid developments in environment friendly air conditioning technologies. With regard to energy use, global warming

* Corresponding author. Tel.: +81-92-583-7832; fax: +81-92-583-7833.
E-mail addresses: bidyutb@cm.kyushu-u.ac.jp (B.B. Saha), kasiwagi@cc.tuat.ac.jp (T. Kashiwagi), mpengkc@nus.edu.sg (K.C. Ng).
[1] Vice President, IIR Commission B1.

0140-7007/03/$35.00
doi:10.1016/S0140-7007(03)00074-4

Nomenclature

A	heat transfer area (m^2)
C_p	specific heat
D_s	surface diffusivity (m^2/s)
D_{so}	pre-exponential constant in Eq. (5) (m^2/s)
E_a	activation energy (J/kg of mole)
k	limiting amount adsorbed (kg/kg)
$k_s a_p$	overall mass transfer coefficient (1/s)
L	latent heat of vaporization (J/kg)
m	mass flow rate (kg/s)
n	parameter in Eq. (1)(–)
$P_S(T)$	saturated vapor pressure (kPa)
q	amount adsorbed (kg water vapor/kg dry adsorbent)
q^*	equilibrium amount adsorbed (kg/kg)
Q_{chill}	cooling capacity (kW)
Q_{hot}	driving heat (kW)
Q_{st}	adsorption heat (J/kg)
R	real gas constant (J/kg of mole K)
R_p	average radius of silica gel (m)
T	temperature (°C)
t	time (s)
U	overall heat transfer coefficient (W/m^2 K)
W	mass (kg)

Subscripts

ad	adsorber/desorber bed of silica gel
ads	adsorption
Al	aluminum
chill	chilled water
cond	condenser
cool	cooling water
Cu	copper
des	desorption
eva	evaporator
ew	liquid refrigerant in evaporator
fHex	fin (aluminum)
Hex	heat exchanger
Hot	hot water
IN	inlet
Khex	heat transfer tube (copper)
OUT	outlet
regen	regeneration
s	adsorbent (silica gel)
w	water
water	Heat transfer fluid
v	water in vapor phase

prevention has been requiring a thorough revision of energy utilization practices towards greater efficiency.

Low temperature sources coupled to a suitable heat pump upgrade heat to a higher temperature. This is achieved by the consumption of electricity (vapor compression heat pumps) or by thermal means (sorption heat pumps). Liquid/vapor heat pumps commonly use $LiBr/H_2O$, which is followed by H_2O/NH_3 as the working fluids. Though vapor compression and absorption heat pumps are common, research in the other category of heat pumps, namely chemical heat pumps including solid/vapor adsorption systems has gained momentum in the last few years [1–3].

Though very high in efficiency, vapor compression cycles are questioned due to environmental problems and the need of electric power to drive the cycles. Compared with thermally driven single-stage $LiBr/H_2O$ absorption chiller, silica gel–water adsorption chiller is a viable competitor. For the former type of chiller, since LiBr solution is corrosive, relatively expensive corrosion resistant alloy steel has to be employed for its construction. For large capacity chiller, a solution pump has to be employed within the chiller circuit. There is also a risk of crystallization. The lowest temperature that can actually be used for generating the said type of chiller, without crystallization, is 61 °C in combination with a coolant inlet temperature at 31 °C. In comparison, silica gel–water adsorption chiller is free of the above mentioned problems.

Waste heat or solar energy driven absorption (liquid–vapor) and adsorption (solid–vapor) systems have the advantage of being environmentally benign: both their ODP (ozone depletion potential) and GWP (global warming potential) are zero. Absorption cycles reach relatively higher performance in comparison with adsorption cycles, but their applications are limited to high and medium temperature heat sources. Adsorption cycles using silica gel–water, active carbon–methanol and charcoal–methanol as the adsorbent–refrigerant pairs have a distinct advantage over other systems in their ability to be driven by heat of relatively low, near-ambient temperatures, so that waste heat below 100 °C can be recovered, which is highly desirable. However, the regeneration temperature range (difference between the highest possible driving source temperature and the lowest possible driving source temperature) of the aforementioned adsorption cycles is small, usually around 30 K.

Adsorption of vapor into silica gel was used in refrigeration equipment in the late 1920s, as reported by Hulse [4]. The silica gel–sulphur dioxide pair was applied to propane-fired, air-cooled cargo train refrigeration system, which was capable of cooling cargo wagons down to −12 °C.

From the 1970s, interest in the solid–vapor systems was rekindled in view of their energy saving potential. A considerable number of studies have been conducted on solid–vapor heat pump systems. The followings are some representative examples. Meunier [5] studied a solid–vapor system using the zeolite–water pair. The

same system was analytically investigated by Douss et al. [6]. Delgado et al. [7], Pons and Grenier [8] and Exell et al. [9] studied the active carbon–methanol system for ice production by using renewable energy. The charcoal–methanol system was investigated by Critoph and Vogel [10] and by Critoph [11] for solar cooling. The silica gel–water system was investigated analytically by Saha et al. [12] and experimentally by Boelman et al. [13] for adsorption cooling.

All the above-mentioned cycles are basic cycles. Advanced cycles are usually designed to attain higher performance. Douss and Meunier [14] proposed and analyzed a cascading adsorption cycle in which an active carbon–methanol cycle is topped by a zeolite–water cycle. The experimental COP reaches 1.06 with driving heat source temperature at around 250 °C. Saha et al. [15] proposed and investigated an advanced, two-stage silica gel–water cycle that can deliver 7 °C chilled water with a hot water at temperature 55 °C in combination with a heat sink (cooling water) at 30 °C. Their COP is low (around 0.33). Sato et al. [16] have analyzed a multi-bed strategy, where heat removal from adsorber is performed by the refrigerant emanating from one or more evaporator(s). It is more practical to have the evaporator devoted to cooling the chilled water, with then evaporated refrigerant being super-heated at the adsorbers. This causes an under-utilization of the sorption elements. Chua et al. [17] have analytically investigated a multi-bed regenerative adsorption chiller. The regenerative chiller improves significantly the waste heat recovery efficiency. However, the chiller is operational with driving source temperature above 60 °C in combination with a coolant at 30 °C.

From the above perspective, the present authors have investigated the performance of a dual mode, three-stage, non-regenerative, and six-bed, regenerative silica gel–water chiller, which can be driven by low temperature waste heat or renewable energy sources in a wide range; between 40 and 95 °C. Two operation modes are possible for the advanced chiller. The first operation mode will be to work as a high efficient conventional chiller where the driving source temperature is between 60 and 95 °C. The second operation mode will be to work as an advanced, three-stage adsorption chiller where the available driving source temperature will be lower than 60 °C (i.e., between 40 and 60 °C).

2. Dual-mode adsorption cycle

2.1. Conceptual Dühring diagram for the innovative cycle

As can be seen from the conceptual Dühring diagram (Fig. 1), the single-stage silica gel–water cycle in multi-bed mode can not operate effectively if the driving heat source temperature is below 60 °C in combination with a coolant at temperature 30 °C or higher, which would likely be the case for an air-cooled cooling tower in summer, in Tokyo. For practical utilization of these temperatures in adsorption chiller operation, an advanced, dual-mode cycle is designed. As can be seen from Fig. 1, the three-stage cycle allows ΔT_{regen} (heat source and heat sink temperature difference) of the adsorbent to be reduced by dividing the condensation-evaporation pressure lift ($P_{\text{cond}}-P_{\text{eva}}$) into three smaller lifts. Refrigerant (water vapor) pressure thus rises into three progressive steps from evaporation to condensation level. In order to attain this objective, the introduction of four additional sorption elements is necessary, as shown in Fig. 3.

2.2. Six-bed regenerative strategy

The proposed six-bed regenerative strategy is an extension from the conventional, two-bed operation. In a conventional adsorption chiller, the inherent restriction in the number of beds resulted in significant temperature fluctuation in all the components. The peak temperature of the condenser outlet that follows shortly after the bed switching adds on to the instantaneous load of the cooling tower. The multi-bed scheme will serve to significantly reduce the peak temperatures in

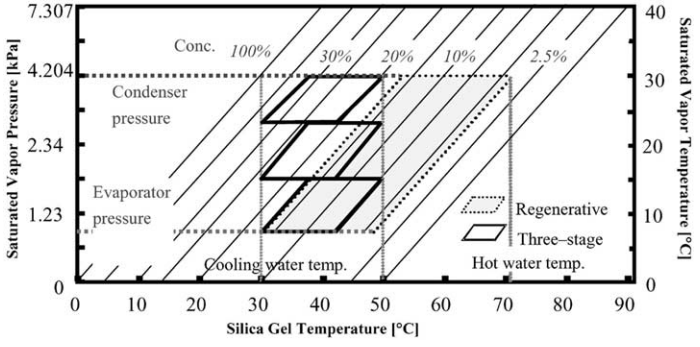

Fig. 1. Conceptual Dühring diagram of the advanced adsorption chiller in dual-mode operations.

both the evaporator and condenser [18]. The second objective is to improve the recovery efficiency of waste heat to useful cooling. Such low temperature, industrial waste heat (typically below 100 °C) is commonly purged into the environment. The enthalpy of such waste heat relative to that of the ambient represents a fixed energy expenditure waiting to be tapped for productive uses. However, such a rigid configuration for the string of adsorption chillers represents an under-utilization of these downstream adsorption chillers. The multi-bed scheme will be shown to eliminate such rigid configurations. Table 1 and Fig. 2 depict the energy utilization schedule and flow configuration for the chiller in six-bed operational mode, respectively. By capitalizing the phase difference between the three pairs of sorption elements, the heat source from the hottest desorber can be used to regenerate another cooler desorber that will act as the intermediate temperature desorber. The outlet hot water from the intermediate temperature desorber will further regenerate the third desorber (low temperature desorber) before being purged into the ambient. Similarly, the coolant from the coldest adsorber can be used in cascaded manner (cooling water outlet from the lowest temperature adsorber to intermediate temperature adsorber

Table 1
Energy utilization schemes for the adsorption cycle in multi-bed mode

Bed 1	Sw	Ads (3)		Ads (2)		Ads (1)		Sw	Des (3)		Des (2)			Des (1)		
Bed 2		Des (1)		Sw	Ads (3)		Ads (2)			Ads (1)		Sw	Des (3)			Des (2)
Bed 3		Des (2)			Des (1)		Sw	Ads (3)			Ads (2)			Ads (1)		Sw Des (3)
Bed 4	Sw	Des (3)			Des (2)			Des (1)		Sw	Ads (3)			Ads (2)		Ads (1)
Bed 5		Ads (1)		Sw	Des (3)			Des (2)			Des (1)		Sw	Ads (3)		Ads (2)
Bed 6		Ads (2)			Ads (1)		Sw	Des (3)			Des (2)			Des (1)		Sw Ads (3)

Ads: bed operating in adsorption mode (adsorber). Des: bed operating in desorption mode (desorber). Sw: switching from adsorber to desorber, and receiving heating stream from heat source or Des ($n/2-1$). Or switching from desorber to adsorber, and receiving coolant from condenser or Ads ($n/2-1$). Here n denotes the total number of beds. $n=6$ in the present case. (1): This refers the situation when the sorption element receives either coolant from the condenser or hot water directly from the heat source. (2): This refers the situation when the sorption element receives hot water from desorber (1) if it is in desorption operation; or receives coolant from adsorber (1) if it is in adsorption mode. (3): This refers the situation when the sorption element receives hot water from desorber (2) if it is in desorption operation; or receives coolant from adsorber (2) if it is in adsorption mode. The width of each box is an indication of the relative time duration over one cycle.

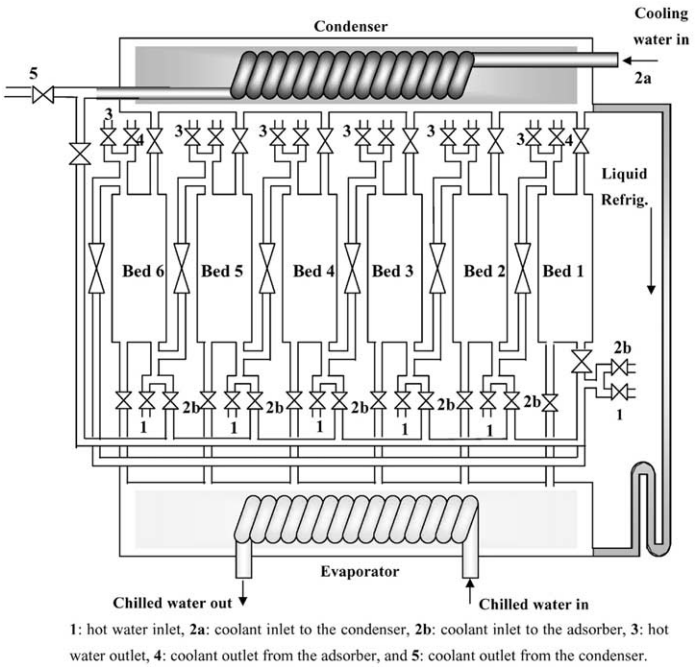

Fig. 2. Schematic diagram of the advanced adsorption chiller in six-bed regenerative operation mode.

from where the coolant outlet enters the high temperature adsorber) before being sent back to the cooling tower.

2.3. Staged regeneration strategy (three-stage operation mode)

If the available heat source temperature is below 60 °C, conventional adsorption chiller is not operational with a coolant of temperature 30 °C or higher. For practical utilization of these temperatures in adsorption chiller operation, staged regeneration is necessary. Fig. 3 illustrates the adsorption cycle in three-stage operation mode. Refrigerant (water), evaporates inside the evaporator, picking up evaporation heat from the chilled water, is adsorbed by adsorber 6 via valve 8. Sorption elements 2 and 4 adsorb refrigerant from desorbers 3 and 5, respectively, via valves 3 and 6. Desorber 1 is connected to the condenser via valve 1. The desorbed refrigerant vapor is condensed in the condenser at temperature T_{cond}; cooling water removes the condensation heat. This condensed refrigerant comes back to the evaporator via the capillary tube connecting the condenser and evaporator to complete the cycle. The capillary tube is bent for achieving a pressure drop resulting in the refrigerant being in liquid phase in the evaporator. The use of parallel cooling water circuits for the condenser and adsorbers 2, 4 and 6 results in similar temperature levels at the condenser (T_{cond}) and those adsorbers (T_{ads}). When refrigerant concentrations in the adsorbers and desorbers are at or near their equilibrium level, the flows of hot and cooling water are redirected by switching the valves so that the desorbers switch into adsorption modes and the adsorbers change into desorption operations. During this short intermediate process no adsorption/desorption occurs. This is needed to pre-heat the adsorbers and pre-cool the desorbers. The resulting low-pressure refrigerant is again adsorbed by the adsorbent to continue the process. During the multistage operation mode, no heat transfer fluid flows through the tubes and valves depicted by broken lines in Fig. 3. The time chart of the chiller in three-stage operation is shown in Table 2.

3. Mathematical modeling

The equation used to describe the silica gel–water properties assume an equilibrium process, without hysteresis, and isobaric adsorption/desorption. The Freundlich equation below, Eq. (1), was chosen for providing a concise analytical expression of experimental data, in the form:

$$q^* = k \cdot [P_s(T_w)/P_s(T_s)]^{1/n} \quad (1)$$

where, q^* is the amount adsorbed in equilibrium. $P_S(T_W)$ and $P_S(T_S)$ are the saturation vapor pressure at water vapor temperature (T_W) and silica gel temperature

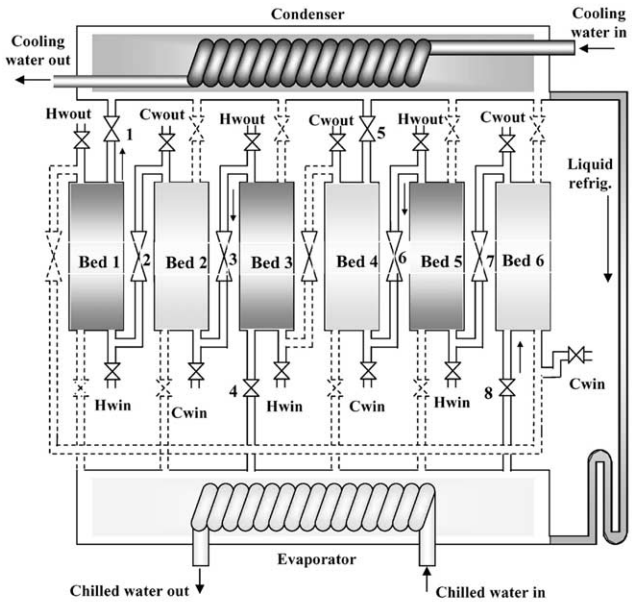

Bed 1: desorber 1, **Bed 2**: adsorber 2, **Bed 3**: desorber 3, **Bed 4**: adsorber 4, **Bed 5**: desorber 5, **Bed 6**: adsorber 6; **1**: valve 1, **2**: valve 2, **3**: valve 3, **4**: valve 4, **5**: valve 5, **6**: valve 6, **7**: valve 7, **8**: valve 8.

Fig. 3. Schematic of the innovative adsorption cycle in three-stage operation mode.

Table 2
Chiller operation time chart in three-stage mode

Cycle		Desorption, Mode A	Pre-heating/ pre-cooling, Mode B	Adsorption, Mode C	Pre-heating/ pre-cooling , Mode D
Time (s)		300	30	300	30
Valve	1, 3, 6, 8 2, 4, 5, 7	Open Closed	Closed Closed	Closed Open	Closed Closed
Sorption element	1, 3, 5 2, 4, 6	Hot water Coolant	Coolant Hot water	Coolant Hot water	Hot water Coolant

(T_S), respectively. By comparing Eq. (1) plots to experimental data obtained from an adsorption chiller manufacturer [19], one of the authors of the current study obtained good agreement only in a relatively narrow pressure and temperature ranges. This led him to modify the Freundlich equation by replacing the constants k and $1/n$ by adjustable parameters $A(T_s)$ and $B(T_s)$ in the following form [20]:

$$q^* = A(T_s) \cdot [P_s(T_w)/P_s(T_s)]^{B(T_s)} \quad (2)$$

where

$$(T_s) = A_0 + A_1 \cdot T_s + A_2 \cdot T_s^2 + A_3 \cdot T_s^3$$
$$B(T_s) = B_0 + B_1 \cdot T_s + B_2 \cdot T_s^2 + B_3 \cdot T_s^3$$

The numerical values of A_0–A_3 and B_0–B_3 are determined by the least square fit to experimental data, which are furnished in Table 3. The values of parameters adopted in the calculation are listed in Table 4.

3.1. Adsorption rate

The adsorption process in an adsorbent bed is considered to be controlled by macroscopic diffusion into the particle bed. The adsorption rate is expressed as Sakoda and Suzuki [21]:

$$dq/dt = k_s a_p (q^* - q) \quad (3)$$

The overall mass transfer coefficient ($k_s a_p$) for adsorption is given by:

Table 3
Values for the parameters used in Eq. (2)

Parameter	Value
A_0	−6.5314
A_1	0.72452×10^{-1}
A_2	$-0.2395l\times10^{-3}$
A_3	0.25493×10^{-6}
B_0	−l5.587
B_1	0.15915
B_2	$-00.5061l2\times10^{-3}$
B_3	0.5329×10^{-1}

$$k_s a_p = \frac{15 D_S}{R_p^2} \quad (4)$$

The surface diffusivity D_s is expressed as:

$$D_S = D_{SO} \cdot \exp\left(\frac{E_a}{RT}\right) \quad (5)$$

Table 4
Values of parameters adopted in the simulation

Symbol	Value	Unit
A_{ad} (area of adsorber)	0.382	m^2
A_{ad} (area of desorber)	0.382	m^2
A_{cond}	0.511	m^2
A_{eva}	0.183	m^2
Cp_{Al}	905	J/kg K
Cp_{Cu}	386	J/kg K
Cp_{water}	4180	J/kg K
Cp_v	1900	J/kg K
Cp_s	924	Jikg K
D_{so}	$2.54\times l0^{-4}$	m^2/s
E_a	4.2×10^4	J/mol
L_w	2.5×10^6	J/mol
m_{water} (coolant flow rate in condenser)	0.34	kg/s
m_{water} (chilled water flow rate)	0.084	kg/s
m_{chill} (chilled water flow rate)	0.084	kg/s
m_{water} (coolant flow rate in adsorbers)	0.57	kg/s
m_{water} (hot water flow rate)	0.57	kg/s
Q_{st}	2.8×10^6	J/mol
R	8314	J/kg of mol K
R_p	$1.7\times l0^{-4}$	m
t_{cycle}	660	s
U_{ad} (overall heat transfer coefficient of each adsorber)	1700	W/m^2 K
U_{ad} (overall heat transfer coefficient of each desorber)	1800	W/m^2 K
U_{cond}	5600	W/m^2 K
U_{eva}	2000	W/m^2 K
W_{ew}	10	kg
W_{fHex}	1.99	kg
W_{kHex}	2.5	kg
W_s	45	kg

During operation, the evaporated refrigerant would nearly simultaneously reach all the silica gel in the adsorber. In such a case, the interparticle resistance approaches to zero and modeling the adsorption/desorption rate for the silica gel–water pair in Eq. (3) is justified. In the present treatment, the effect of the refrigerant mass in the gas phase is ignored.

3.2. Mass balance

The mass balance of refrigerant (water) is written by neglecting the gas phase as:

$$\frac{\mathrm{d}Ww}{\mathrm{d}t} + W_s\left(\frac{\mathrm{d}q_{des}}{\mathrm{d}t} + \frac{\mathrm{d}q_{ads}}{\mathrm{d}t}\right) = 0 \tag{6}$$

3.3. Adsorption and desorption energy balances

Neglecting the dependence of specific heat on temperature and of adsorption heat on concentration the adsorption and desorption energy balances are described by the following equations:

$$T_{waterOUT} = T_{ad} + (T_{waterIN} - T_{ad}) \cdot \exp\left(\frac{-U_{ad} \cdot A_{ad}}{m_{water} \cdot Cp_{water}}\right) \tag{7}$$

$$\frac{\mathrm{d}}{\mathrm{d}t}\{W_s(Cp_s + Cp_w \cdot q) + (Cp_{Cu} \cdot W_{kHex} + Cp_{Al} \cdot W_{fHex})\} \cdot T_{ad} = Q_{st} \cdot W_s \cdot \frac{\mathrm{d}q}{\mathrm{d}t} + m_{water} \cdot Cp_{water}(T_{waterIN} - T_{waterOUT}) - \delta \cdot W_s \cdot Cp_v(T_{ad} - T_{eva}) \cdot \frac{\mathrm{d}q}{\mathrm{d}t} \tag{8}$$

where

$$\delta = \begin{cases} 1 & \text{if the bed is in adsorption mode,} \\ 0 & \text{if the is in desorption mode.} \end{cases}$$

For adsorption energy balances, the subscripts water and ad denote cooling water and adsorber, respectively; for desorption, they denote hot water and desorber, respectively.

The left hand side of the adsorber/desorber energy balance equation [Eq. (8)] provides the amount of sensible heat required to cool or heat the adsorbent (s), the water (w) as well as heat transfer tube (Cu) and fin (Al) parts of the sorption element during adsorption and desorption. The first term on the right hand side of Eq. (8) represents the release of adsorption heat during adsorption process or the input of desorption heat during desorption operation. The second term on the right hand side of Eq. (8) indicates the total amount of heat released to the cooling water upon adsorption or provided by the hot water for desorption. The last term accounts for the amount of heat needed to superheat the incoming refrigerant vapor from the evaporation temperature (T_{eva}) to adsorption temperature (T_{ads}).

3.4. Evaporator and condenser energy balances

For the energy balances in the evaporator and condenser, the following expression are used:

$$T_{waterOUT} = T_{ad} + (T_{waterIN} - T_{ad}) \cdot \exp\left(\frac{-U_{eva,cond} \cdot A_{eva,cond}}{m_{water} \cdot Cp_{water}}\right) \tag{9}$$

$$\frac{\mathrm{d}}{\mathrm{d}t}\{(Cp_w \cdot W_{ew} + Cp_{Cu} \cdot W_{eva,cond})T_{eva,cond}\} = -L_w \cdot W_s \cdot \frac{\mathrm{d}q_{des,ads}}{\mathrm{d}t} + m_{water} \cdot Cp_{water}(T_{waterIN} - T_{waterOUT}) + Cp_{water,v} \cdot W_s \cdot \frac{\mathrm{d}q_{des}}{\mathrm{d}t}(T_{cond,des} - T_{eva,cond}) \tag{10}$$

In Eqs. (9) and (10), the subscripts water and eva denoting chilled water and evaporator, respectively, for the evaporator heat balances. For the condenser heat balances, they denote cooling water and condenser, respectively. The subscript ew denotes the amount of liquid refrigerant inside evaporator. For condenser energy balance the value of ew is taken as zero.

3.5. COP and cooling capacity (Q_{chill})

The COP and cooling capacity are defined by the following equations:

$$COP = Q_{chill}/Q_{hot} \tag{11}$$

$$Q_{chill} = m_{chill} \cdot Cp_{water} \cdot \int_0^{t_{cycle}} (T_{chillIN} - T_{chillOUT})\mathrm{d}t \tag{12}$$

where

$$Q_{hot} = m_{hot} \cdot Cp_{water} \cdot \int_0^{t_{cycle}} (T_{hotIN} - T_{hotOUT})\mathrm{d}t$$

Here t_{cycle} denotes the total cycle time.

3.6. Simulation procedure

The system of differential Eqs. (2)–(10) was solved simultaneously by numerical integration using finite difference substitution in the derivatives. In the simulation, temperature is assumed to be uniform along the heat exchanger. The simulation procedure for the multi-stage operation mode is almost analogous to that of the conventional cycle [12]. However, the calculation procedure is slightly modified to accommodate three nested-loop

iterations to perform, instead of one by which the convergence is obtained for each of the six sorption elements. The convergence factor is taken as 10^{-3} for all parameters. The calculations are made with a time interval of one second.

4. Results and discussion

To clarify the practical operational limits and also the performance characteristics, cycle simulation runs were performed for the dual-mode, regenerative multi-bed and non-regenerative multi-stage chiller. Since the main objective is to use low temperature waste heat (below 100 °C) as the driving source, the investigation was conducted for hot water temperature between 40 and 95 °C.

4.1. Cooling water temperature

Figs. 4(a) and (b) show the effect of cooling water temperature on cooling capacity and COP. Hot water inlet temperature is chosen as 80 and 50 °C for regenerative multi-bed and non-regenerative multi-stage operation, respectively. Chilled water inlet temperature is taken as 12 °C. For both the multi-bed and multi-stage operations, cooling capacity increases as the cooling water temperature is lowered. This tendency results because the lower adsorption temperature causes higher amount of refrigerant being adsorbed and desorbed during each cycle. It is noteworthy to mention that the innovative chiller is operational with driving heat source temperatures between 40 and 60 °C with a coolant inlet at 30 °C in the three-stage operation mode.

For the multi-bed mode, COP decreases as the coolant temperature increases. The decreasing rate of COP is very significant for cooling water temperatures between 35 and 40 °C in combination with a heat source at 80 °C. This indicates that for a fixed temperature driving source, there is an operating temperature limit of the cooling water in the multi-bed operation mode.

4.2. Hot water temperature

Fig. 5(a) shows the effect of hot water temperature on cooling capacity. When the available driving source temperature is at or above 60 °C, the chiller should be changed from multi-stage operation mode to multi-bed operation mode to attain higher performance. For a fixed coolant temperature of 30 °C, cooling capacity increases moderately as the hot water temperatures increase from 40 to 55 °C in the three-stage operation. Cooling capacity decreases for heat source temperatures between 55 and 60 °C due to the heat losses in multi-stage operation. For the multi-bed operation mode, cooling capacity increases significantly with the whole range of driving source inlet temperatures studied here. This is because the increased amount of refrigerant desorption with higher driving source temperature.

The effect of hot water temperature on COP is shown in Fig. 5(b). The COP peaks at around 50 °C for the three-stage operation, while the COP increases sharply with the hot water inlet temperature between 60 and 70 °C for the multi-bed operation mode. For the driving

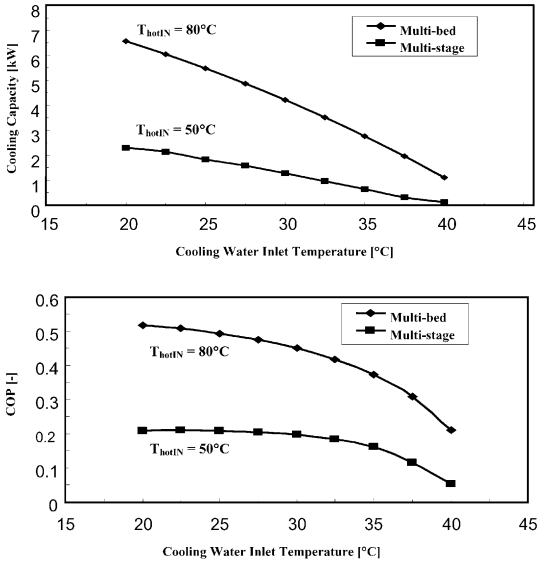

Fig. 4. (a). Cooling water temperature effect on cooling capacity; (b) cooling water temperature effect on COP.

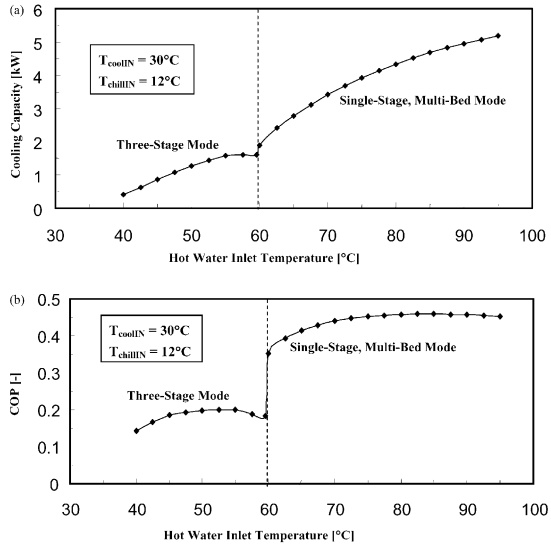

Fig. 5. (a). Hot water temperature effect on cooling capacity; (b) hot water temperature effect on COP.

source inlet temperature above 70 °C, the COP improvement is marginal.

5. Conclusions

The practical operational limits and performance characteristics with near-ambient temperature heat sources and small regenerating temperature lifts were investigated for the dual-mode, multi-stage, multi-bed regenerative adsorption chiller. The main conclusions are as follows:

1. The main advantage in the innovative dual-mode cycle is its ability to utilize effectively low grade waste heat of temperature between 40 and 95 °C as the driving heat sources.
2. The chiller in the three-stage mode is operational with a heat source and heat sink temperature difference as small as 10 K.
3. With relatively higher driving source temperatures (above 60 °C), the chiller in regenerative multi-bed mode yields higher performance.
4. The cycle in both modes is more sensitive to heat sink temperature than to heat source temperature.
5. From the above perspectives, the use of unexploited waste heat at near-ambient temperature may offer attractive possibilities for improving energy efficiency.

Acknowledgements

This work was financially supported by International Joint Research Grant OIGPI of the New Energy and Industrial Technology Development Organization (NEDO).

References

[1] Meunier F. Solid sorption: an alternative to CFCs. Heat Recovery Systems and CHP 1993;13(4):289–95.
[2] Spinner B. Ammonia-based thermochemical transformers. Heat Recovery Systems and CHP 1993;l3(4):301–7.
[3] Saha BB, Akisawa A, Kashiwagi T, Ng KC, Chua HT. Heat driven heat pumps for the 21st century. In: Proceedings of the JSPS and NUS/NTU Seminar, Singapore, 2000. p. 397–406.
[4] Hulse GE. Refroidissement d'un wagon frigorifique a merchandises par un systeme a adsorption utilisant le gel de silice. Revue Generale de Froid 1929;10:281–7.
[5] Meunier F. Utilisation des cycle a sorption pour la production de froid par l'énergie solaire. Cahiers de l'AFEDES 1978;5:57–67.
[6] Douss N, Meunier F, Sun LM. Predictive model and experimental results for a two adsorber solid adsorption heat pump. Ind Eng Chem Res 1988;27:310–6.
[7] Delgado R, Choisier A, Grenier P, Ismail I, Meunier F, Pons M. Etude de cycle intermittent charbon actif-methanol en vue de la realisation d'une machine a fabriquer de la glare fonctionnant a l'energie solaria. In: Proc. Meeting of IIR Commissions El-E2, Jerusalem, Israel 1982. p. 185–91.
[8] Pons M, Grenier P. Experimental data on a solar powered ice maker using active carbon and methanol adsorption pair. Carbon 1986;24:615–25.
[9] Exell RHB, Bhattacharya SC, Upadhyaya YR. Research and development of solar powered desiccant refrigeration for cold storage application. Bangkok: Asian Institute of Technology; 1993 [AIT research report no. 265].
[10] Critoph RE, Vogel R. Possible adsorption pairs for use in solar cooling. Int J Ambient Energy 1986;7(4):183–90.
[11] Critoph RE. Performance limitations of adsorption cycles for solar cooling. Solar Energy 1988;4l:21–30.
[12] Saha BB, Boelman EC, Kashiwagi T. Computer simulation of a silica gel–water adsorption refrigeration cycle—the influence of operating conditions on cooling output and COP. ASHRAE Transactions 1995;39(2):348–57.
[13] Boelman EC, Saha BB, Kashiwagi T. Experimental investigation of a silica gel–water adsorption refrigeration cycle—the influence of operating conditions on cooling output and COP. ASHRAE Transactions 1995;39(2):358–66.
[14] Douss N, Meunier F. Experimental study of cascading adsorption cycles. Chemical Engineering Science 1989; 44(2):225–35.
[15] Saha BB, Alam KCA, Akisawa A, Kashiwagi T, Ng KC, Chua HT. Two-stage non-regenerative silica gel–water adsorption–refrigeration cycle. Proceedings of the ASME Advanced Energy Systems Divisions, Orlando, USA 2000; 40:65–9.
[16] Sato H, Tanaka H, Honda 5, Fujiwara K, Inoue S. Adsorptive type refrigeration apparatus. US patent no. 5775126, 1998.
[17] Chua HT, Ng KC, Malek A, Kashiwagi T, Akisawa A, Saha BB. Multi bed regenerative adsorption chiller-improving the utilization of waste heat and reducing the chilled water outlet temperature fluctuation. International Journal of Refrigeration 2001;24:124–36.
[18] Chua HT, Ng KC, Malek A, Kashiwagi T, Akisawa A, Saha BB. Multi-reactor regenerative adsorption chiller. Singapore patent no. 9804792-1, 1999.
[19] Nishiyodo Air Conditioning Company Ltd. PTX data for the silica gel–water pair. Manufacturer propriety data, 1992.
[20] Saha BB. Performance analysis of advanced adsorption cycle. PhD thesis, Tokyo University of Agriculture and Technology, 1997.
[21] Sakoda A, Suzuki M. Fundamental study on solar powered adsorption cooling system. Journal of Chemical Engineering Japan 1984;17(1):52–7.